

ADVANCED EDUCATION AND RESEARCH ON MARINE PROPULSION

-EXPERIMENTAL STUDY ON PROPELLER AIR-DRAWINGS AND BEARING FORCES

Makoto Uchida

Professor, Dr.
Faculty of Maritime Sciences, Kobe University
5-1-1 Fukae-Minami, Higashinada, Kobe
658-0022 Japan
Email: uchida@maritime.kobe-u.ac.jp
Tel: +81-78-431-6295
Fax: +81-78-431-6367

Yuuki Matsumoto

Mizushima Works and Shipyard, Sanoyas Hishino Meisho Co. Ltd.
Katsunori Teshima
Graduate Student of Master's Degree Program
Division of Maritime Sciences,
Graduate School of Science and Technology, Kobe University

Abstract Marine screw propeller is one of the fluid-dynamic propulsor, so the generated thrust is determined by the product of the mass of fluid and the acceleration. When a certain thrust is generated, it is well known on the momentum theory that the greater mass and the lower acceleration of concerned fluid, the better propeller efficiency. Therefore, a larger diameter and a lower rotational speed have been pursued for marine screw propellers; accordingly the propeller immersion depth has been relatively smaller. Even if a propeller blade dose not appears above water surface, an amount of air is drawn from free water surface to the low pressure region on the blade surface and the propeller shaft exciting forces, namely the bearing forces are induced under a certain condition.

In order to investigate the relation between the air-drawing phenomena and the induced bearing forces, the experiments of model propeller in open condition are carried out at the circulating water channel of Kobe University, Faculty of Maritime Sciences (KUMS). The air-drawing phenomena are observed dynamically by using of a high speed video recorder system. The shaft forces (the thrust, the torque and the bearing forces) are detected by the 4 components load cell and analyzed.

Keywords screw propeller; air-drawing; bearing force; shaft force; immersion depth

0 Introduction

A marine screw propeller working near free water surface draws air onto the blade surface under a certain operational condition and a certain volume of cavity is formed on the blade surface. The occurrence of the air-drawing induces the deterioration of the propeller performance and the increase of the fluctuation loads and forces on the propeller shaft. Siba^[1] revealed the fundamentals of the air-drawing phenomena as a pioneering investigation. Nisikawa, et al^[2-4] carried out experimental study and revealed the air-drawing can be classified into the partial air-drawing which is defined unstable and/or partial cavity formed on the blade surface, and the full-drawing which is defined as stable sheet cavity formed over the whole blade surface. And it was also pointed out that the bearing force which is the perpendicular force to the shaft axis increases remarkably when the partial air-drawing occurs. However, the both of cavity variations in time and in space were not been discussed individually, and also the unstable bearing force was considered only from the viewpoint of time averaged analysis in the former investigations^[3, 4].

The dynamic observations of the cavity formation on the propeller blades by using of a high speed video camera and the shaft force measurements are carried out in order to analyze dynamically the partial air-drawing phenomena in this paper.

1 Experimental apparatus and procedure

The experiments were carried out using the circulating water channel in KUMS with 1.2m depth, 1.5m width and 5.5m length of the working section. The open propeller dynamometer which can detect 4 components of the propeller forces and moments was installed on the elevator so as to vary the propeller location to any desired immersion depth. The 4 components, which are the thrust " F_X ", the torque " M_X ", the horizontal bearing force " F_Y " and the vertical bearing force " F_Z " under the still space coordinates, and the rotational phase angle were recorded on the data recorder with 2,000Hz sampling frequency. The visual observations were carried out and recorded by the high speed video camera with 250 frames an second. The measurements and the observations were done under steady flow velocity, steady rotational speed and steady immersion depth. The schematic diagram of experimental apparatus is shown in Fig.1. The principal particulars of examined propeller and the experimental conditions are shown in Table 1 and 2 respectively.

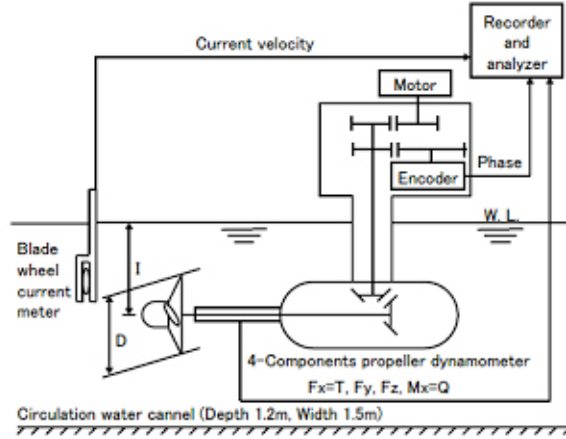


Fig. 1 The schematic diagram of experimental apparatus

The operational conditions are represented as the “ ps ” which is product of the pitch ratio “ p ” and the slip ratio “ s ”. It is in direct proportion apparently to the attack angle of the propeller blade, consequently it means the propeller load amplitude. The propeller immersion depth “ I ” is been dimensionless “ I/D ” by the propeller diameter “ D ”. “ $I/D=0.5$ ” means that the propeller tip at the upper position coincides with the still water surface. The bearing force is valued as the difference between maximum and minimum during one propeller rotational period. The propeller bearing forces are also been dimensionless by an ordinary manner.

$$K_{Fy} = \frac{F_Y}{\rho n^2 D^4}, \quad K_{Fz} = \frac{F_Z}{\rho n^2 D^4} \quad (1)$$

2 Experimental results

2.1 Bearing force measurement

The time averaged bearing force is obtained as a mean value of bearing force over the measured period of about 30 seconds. The fluctuating one is defined as the difference between maximum and minimum values over the same measured period. The bearing force coefficients arranged with I/D are shown by each “ ps ” in Fig.2. The polygonal line shows the time averaged bearing force and the vertical line segments represent the fluctuating amplitude of the bearing force.

The results in terms of the time averaged bearing force agree properly with the former investigations^[3, 4]. An unique change of the time averaged bearing force by the I/D can be seen between $ps=0.7$ and 0.5 . The time averaged bearing force is pretty large in the restricted range of I/D despite the fluctuating one is extremely small.

The all results of bearing force measurements are re-arranged to a contour chart shown in Fig.3 and Fig.4. It can be cleared from Fig. 4 that an unstable air-drawing phenomena is occurred in the narrow region of $1.0 > ps > 0.7$ and $0.75 > I/D > 0.6$.

2.2 Air-drawing observation

The cavity formed on the propeller blades, caused by the air-drawings, is classified into 4 modes

as shown in Fig.5. The first is non-cavity on the any blade, the second is unstable cavity formed and the third is uniformed cavity on the all blades without regard to allover the blades' surface. The fourth indicates there is remarkable difference of cavity formation on the several blades even if it is stable in time. The non-uniformed air-drawing, the fourth mode, can be in addition classified into 4 patterns of which the large cavities are formed on the only one blade, the continuous two blades, the alternate two blades or the continuous three blades compared with the other blades in the case of 4 blades propeller.

The high speed recorded video is played back with slow motion and the cavity formations are evaluated as shown in Fig.6 according to the above definitions.

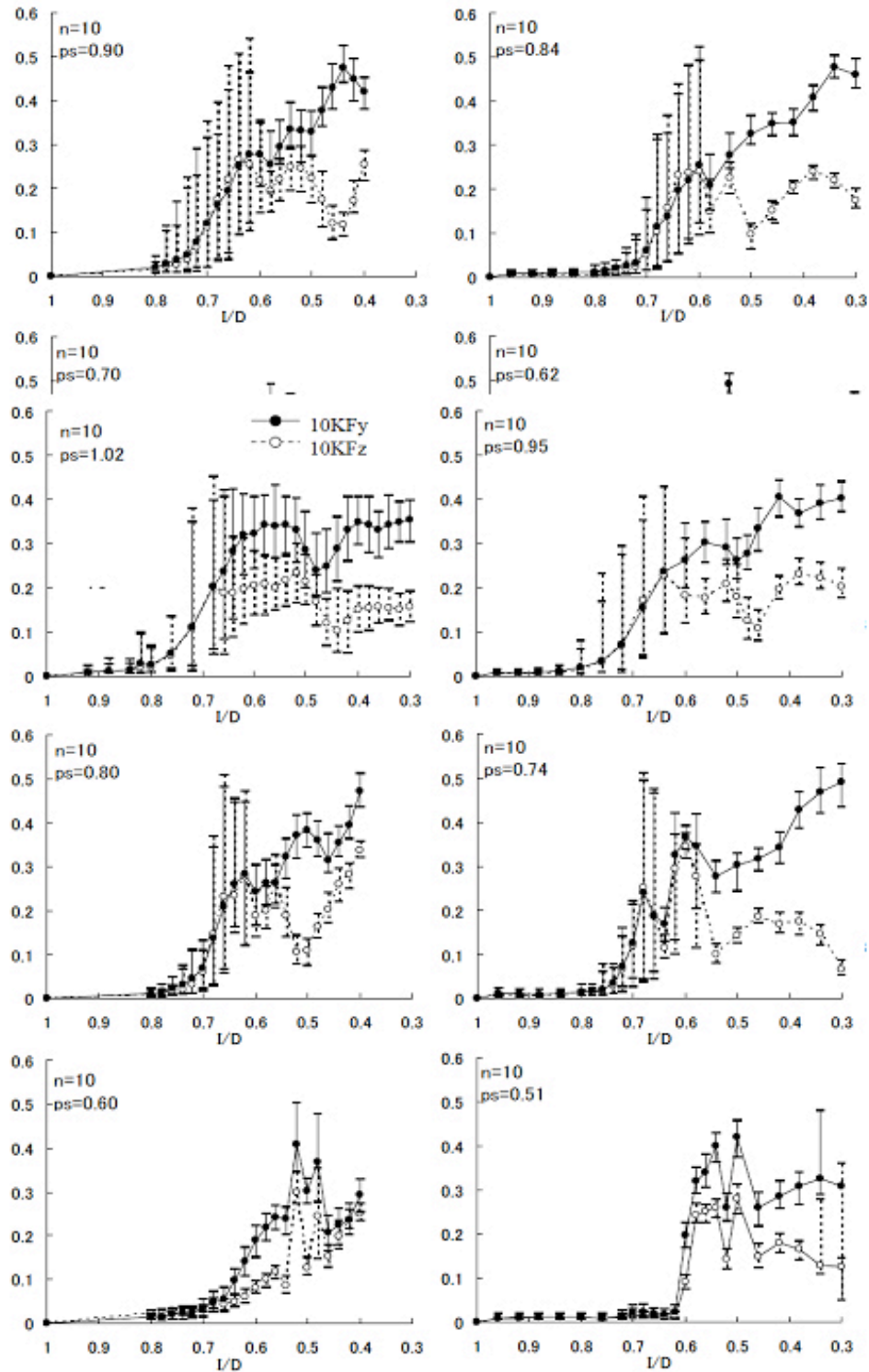


Fig. 2 Bearing force coefficients, K_{Fy} and K_{Fz} , by immersion depth L/D

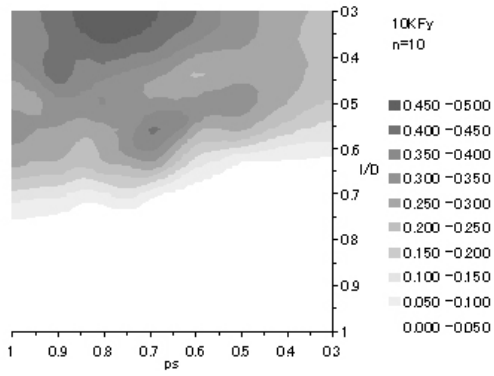


Fig. 3 Contour of the averaged bearing force

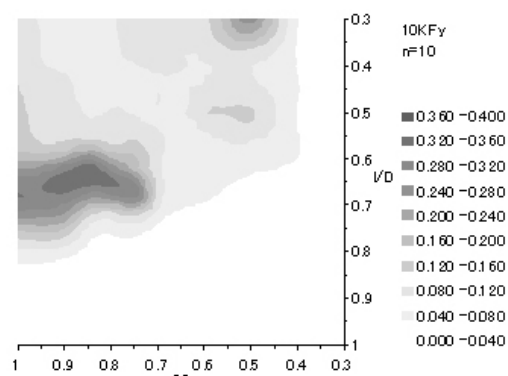


Fig. 4 Contour of the fluctuating bearing force

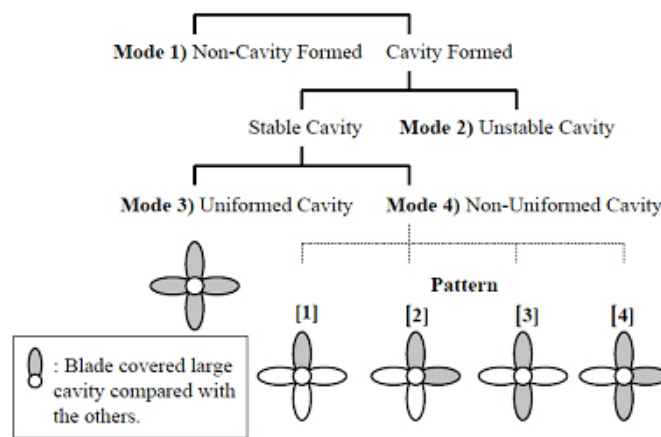


Fig. 5 Classification of cavity formation mode

3 Considerations

3.1 Relation between air-drawing and bearing force

From the results of the averaged bearing force and the cavity formation, i.e. Fig.3 and Fig.7, it can be seen that the steep rise in the averaged bearing force occurs in the region of the non-uniformed air-drawing. The region is insular shape within $0.75 > ps > 0.45$ and $0.7 > I/D > 0.45$.

From the results of the fluctuating bearing force and the cavity formation, i.e. Fig.4 and Fig.7, it can be said the large fluctuation of the bearing force occurs in the region of the unstable air-drawing and the undefined mode. Though the cavity formations in the undefined mode were not able to be confirmed by VTR due to the turbulent bubble around the blade, most undefined mode can be judged as the unstable air-drawing.

3.2 Evaluation chart for air-drawing

The evaluation chart for the air-drawing mode is introduced as shown in Fig.8 by putting together the whole of the results mentioned above. The uniformed air-drawing is divided by the cavity size on the blade into the uniformed full and partial air-drawing. The full is 76%–100% cavity area on the blade, and the partial is under them.

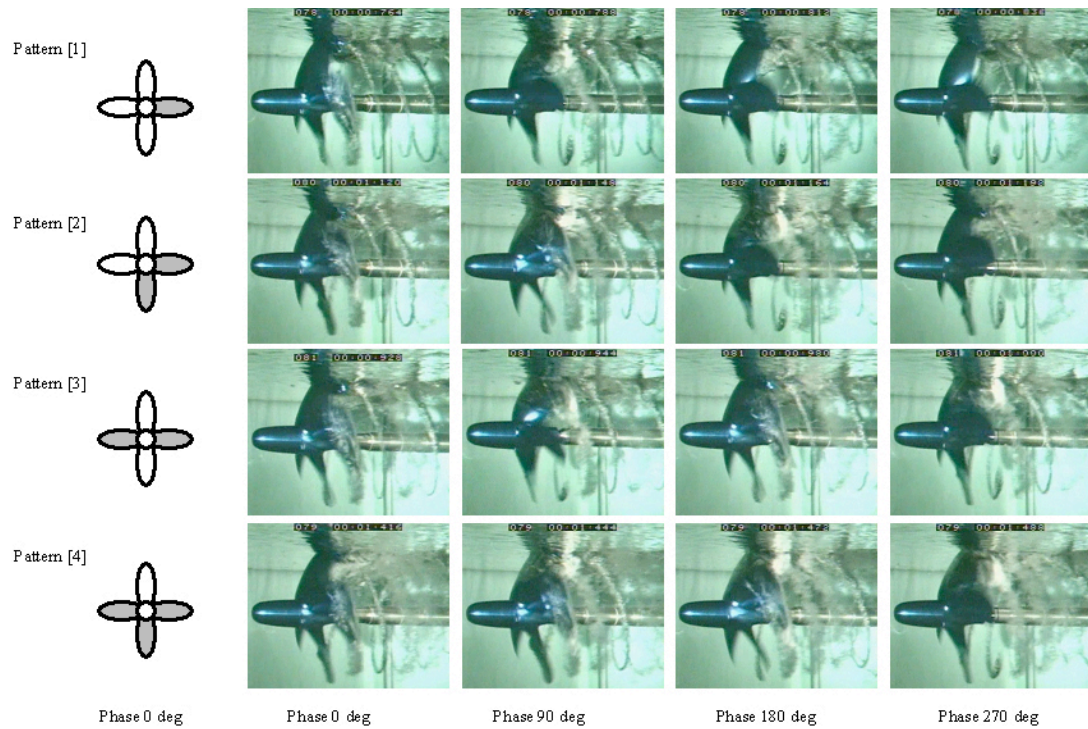


Fig. 6 Typical example of non-uniform air-drawing

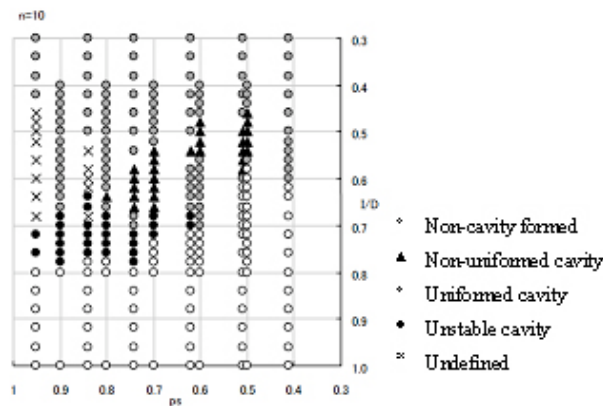


Fig. 7 Results of cavity formation

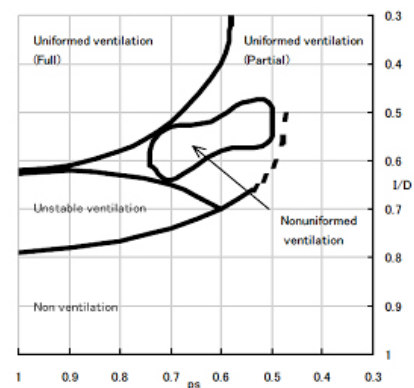


Fig. 8 Evaluation chart for air-drawing mode

The “partial air-drawing” called so far is consist of 3 different modes. They are the uniformed but partial, the non-uniformed and the unstable air-drawing.

3.3 Magnitude of bearing force and pattern of non-uniformed cavity

When the non-uniformed cavities are developed on the blades, the induced bearing forces are increased. Each magnitude of averaged bearing forces on the non-uniformed air-drawing is shown in Fig.9 being assorted into the four cavity formation patterns. The magnitude of bearing force has a strong correlation with the asymmetrical cavity formation. Since the pattern 2 has a largest asymmetry and the pattern 3 has contrastively symmetry, the pattern 2 is highest and the pattern 3 is lowest as respects the magnitude of bearing force.

$$\text{Pattern (2)} > \text{Pattern (4)} > \text{Pattern (1)} \gg \text{Pattern (3)} \quad (2)$$

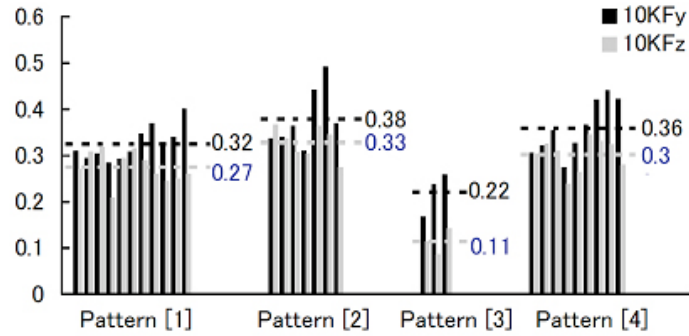


Fig. 9 Averaged bearing forces on non-uniformed air-drawing

Table 1 The principal particulars of examined propeller

Type	MAU
	4-55
Blade number Z	4
Diameter (m) D	0.25
Pitch ratio p	1.1
D.A.R.	0.55
Boss ratio	0.18
Thickness ratio	0.05
Mean width ratio M.W.R.	0.263
Raked angle (deg)	10

Table 2 The experimental conditions

Blade number Z	4	
Diameter (m) D	0.25	
Propeller revolution (rps) n	9	10
Froude number Fn	1.44	1.60
Reynolds number ($\times 10^{-5}$) Re	4.94	5.49
Reynolds number \times M.W.R. ($\times 10^{-5}$)	1.30	1.45
Weber number We	131	146
Advance velocity (m/s) V_a	0.25 – 1.75	
Advance ratio J	0.11 – 0.78	0.10 – 0.70
Slip ratio s	0.90 – 0.29	0.91 – 0.36
Pitch ratio \times Slip ratio ps	0.99 – 0.32	1.00 – 0.40
Depth (m) l	0.25 – 0.075	
Immersion depth ratio l/D	1.00 – 0.30	

4 Conclusion

In order to investigate the relation between the air-drawing phenomena and the induced bearing forces, the experiments of model propeller are carried out. The experimental results obtained in this paper are summarized as follows.

- (1) The cavity formation on the a propeller blades caused by air-drawing is classified into stable or unstable mode, and uniformed or non-uniformed mode. The uniformed air-drawing is also classified by cavity dimension on the blade. The non-uniformed air-drawing is also classified into 4 patterns in the case of 4 blades propeller. It is revealed that the partial air-drawing called so far can be sub-divided into more than one condition.
- (2) The air-drawing can be pigeonholed by immersion depth l/D and ps witch means propeller load. The evaluation chart for air-drawing mode is obtained. The non-uniformed air-drawing can be seen in the confined region on the evaluation chart.
- (3) When the non-uniformed air-drawing occurs, the magnitude of the time averaged bearing force is extremely large, on the other hand the fluctuating bearing force is just little. This means the non-uniformed air-drawing phenomenon is highly stable.
- (4) The magnitude of bearing force at the non-uniformed air-drawing has a strong correlation with

the asymmetrical cavity formation.

Reference

- [1] Shiba H. Air-drawing of Marine Propellers. Report of Transportation Technical Research Institute, 1953(9).
- [2] Hashimoto J, Nishikawa E, et al. An Experimental Study on Propeller Air Ventilation and Its Induced Vibratory Forces. Bulletin of Marine Engineering Society in Japan, 1983(11)1.
- [3] Nishikawa E, Uchida M. An Experimental Study on the Ventilation of Marine Propeller and Its Effects of the Propeller Performance and Shaft Force. Proc of 4th International Symposium on Practical Design of Ships and Mobile Units, 1989(1).
- [4] Nishikawa E, Fujiyama A, Uchida M, et al. Propeller Air Drawing and Its Induced Vibratory Forces—2nd Report. Journal of the Marine Engineering Society in Japan, 1990(28): 8 (Written in Japanese).